I J C T A, 9(2-A), 2016, pp. 435-451

Modeling and Simulation of Energy Conversion System Used in Electric Vehicle

S. Farhani[1], **M. Amari**[2] **and F. Bacha**[3]

ABSTRACT

This paper presents design, modeling and simulation of energy conversion system for electric vehicle. The necessary energy to move the vehicle is provided by two separate energy sources, which are fuel cell and a super capacitor. A high frequency DC-DC converter fed by fuel cell is analyzed. The mathematical model of the fuel cell is presented and the average model of the DC-DC converter is elaborated. The implementing concept of the Field-Oriented speed controller and the PWM inverter technique are illustrated for Permanent Magnet synchronous Motor PMSM. The proposed system control mechanisms are digitally simulated using the MATLAB/ Simulink/ Sim Power Systems software. The dynamic performances of the electric vehicle drives are examined for the standardized European speed cycle type.

Keywords: Electric vehicle; fuel cell; super capacitor; permanent magnet synchronous motor (PMSM); DC-DC converter; vector control.

1. INTRODUCTION

The problems related to the supply of oil, pollution and the greenhouse effect justify the need to develop new technologies for the transportation as a replacement for the actual technology based on internal combustion engines. Fuel cells promise that the best pace that they operate more efficiently and with fewer emissions.

A hybrid propulsion system, which combines two sources:

- Fuel cell is the main source. It is the electrochemical device that converts the chemical energy of a reaction directly into electrical energy. The stack has a slow dynamics done allowing him to answer to an increase or a rapid decrease in the output power as well as the recovery of the energy.
- The super-capacitor is the source of storage; it has significant capacity but a low voltage. It can restore the energy more quickly as a battery. It presents the following advantages:
  - Provide additional power rapid during peak periods such as the acceleration
  - Enable the recovery of the braking energy by the recovery and store it in the super-capacitor, thus increasing the overall efficiency of the vehicle.

The adaptation of the levels of the voltage between the two sources and the load in the vehicle requires two converters DC-DC, the Boost and the Buck-Boost to maintain constant the voltage of the DC bus allowing imposing the power or the current required by the load [1]-[3]-[9].

The other converter is an inverter, it is used to adapt the voltage levels between the DC link and the PMSM (Permanent Magnet Synchronous Motor). In the stationary state, the fuel cell stack must produce

[1,2,3] Laboratory of Computer for IndustrialSystems, ENSIT, University of Tunisia, *Email: farhani.esstt@yahoo.fr, mansour.amari@gmail.com, faouzi.Bacha@esstt.rnu.tn*

the energy required to move the electric vehicle. The fuel cell will become the primary energy source for the next generation of hybrid electric vehicles [15].

This paper deals with the modeling of the elements of the electrical vehicle. This paper begins with a presentation of the energy conversion system of the vehicle. A focus is made on the energy performance of the conversion system. Then, we determine the power required to move the vehicle, while specifying the different forces that act on the vehicle. A large part of this paper is devoted to the modeling and the selection of the electric motor is associated with the vehicle. We propose in this paper an approach for sizing of the fuel cell (number of cells, the surface of a cell and power) and the pack of super capacitor (the number of cells in series, number of cells in parallel, capacity and voltage of a cell) while taking into account of a cycle of conduct standardized[17]-[18].

In this paper we focused on the design and modeling of different converters of power dedicated to electric vehicles. The vehicle considered requires three static converters. The first converter is of the unidirectional DC-DC interface the fuel cell of stack and the DC bus. It is unidirectional and it is constituted by two bridges associated with two planar transformers operating at high frequency: The first bridge is ordered, it works in inverter mode. The second bridge is to diodes, running in rectifier mode. The second associated converter to the super- capacitors is bi-directional and it is composed by two bridges switches. An average model means in small signals has been established for each of the DC-DC converter, in order to determine the transfer function linking the voltage of the DC bus and the duty cycle control of the DC-DC converter. The third converter interfaces the DC bus and the permanent magnet synchronous motor, which the control strategy is the Space Vector PWM technique.

2. ENERGY CONVERSION SYSTEMUSED IN ELECTRIC VEHICLE

The considered electrical vehicle uses a fuel cell as the principal energy source to ensure the average power required by the vehicle. It is connected to the DC bus via anDC/DC unidirectional converter. Packs of the super capacitor in addition to the fuel cell are necessary to ensure obtaining the maximum power on the one hand, (at the accelerations mode) and on the other hand recovering the kinetic energy during the braking phase. This aims is to minimizing hydrogen quantity consumed by the fuel cell. To adjust the voltage level of the super capacitor to that of DC bus, a bidirectional DC/DC converter is inserted between the pack of the super capacitor and the DC bus. The traction of vehicle is achieved through the permanent magnet synchronous motor associated with a three-phases inverter its voltage supply is ensured by the DC link (Fig. 1) [1, 7, 16, 20]. Some recent control methods are discussed in [23-25].

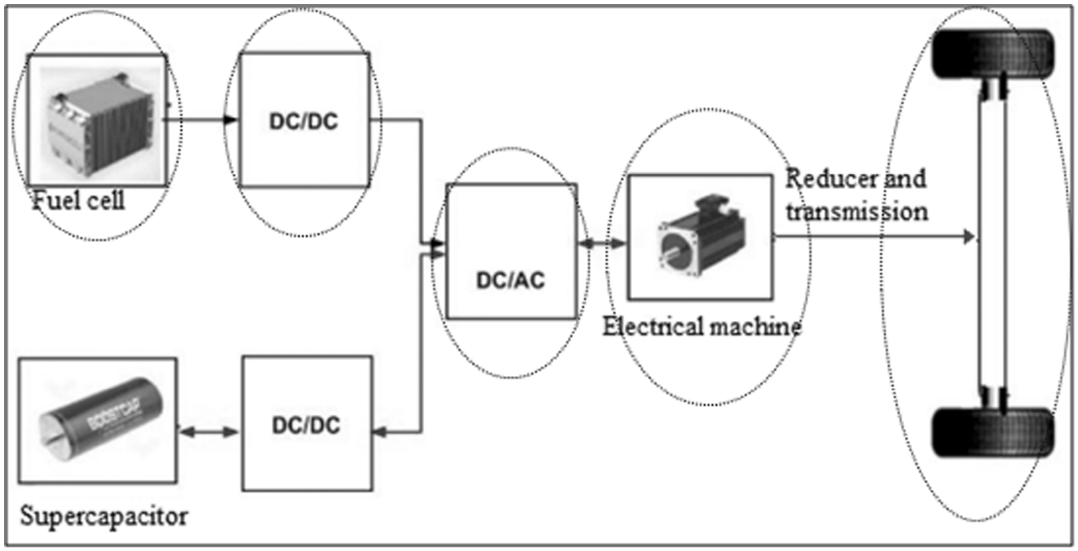

Figure 1: Theenergy conversion system

3. DYNAMICS OF THE VEHICLE

Based on principles of vehicle mechanic, the various forces and the moving vehicle are presented in Fig. 2.

Three main resistances forces $\mathbf{F_A}$, $\mathbf{F_X}$ and $\mathbf{F_R}$ called respectively aerodynamic force, rolling resistance force and gravity force. The tensile force F_X propels the vehicle forward. The propulsion system (the permanent magnet synchronous motor) must provide the necessary force to the vehicle traction at the wheels. This force must firstly provide the necessary effort to speed and partly overcome the resistant force to the coil, the aerodynamic force and road inclination[15].

- Rolling resistance force: The rolling resistance force acts on the level of tires and is opposed to the free movement of the vehicle. It is caused by the deformation of the tires on the road way which generates a rolling friction. It depends on the vehicle mass M (kg), the acceleration of gravity g (m.s-2) and the rolling resistance coefficient C_R.

$$F_R = MgC_R \tag{1}$$

  The gravity force affects immediately the vehicle on the slope. It retains it in rise and pushes it in descent. It depends on the inclination of the slope and the vehicle mass M.

$$F_G = Mg\sin(\theta) \tag{2}$$

- Aerodynamic Force: This is the air resistance force. It varies depending on the vehicle speed and depends on non-linear phenomena within the fluid mechanics. It is proportional to the air density ñ (Kg/m^3), to the front section Sf (m^2) of the vehicle, the drag coefficient Cx of the air and vehicle speed V (ms-1).

$$F_A = \frac{\rho C_x S_f V^2}{2} \tag{3}$$

- Traction force: It indicates the force which is exerted on the periphery of the driving wheels in contact with the ground to create or maintain the movement of the vehicle. The magnitude force depends on the motor torque, gear transmission and the radiusof the wheels.

$$F_x(t) = M\frac{dV(t)}{dt} + Mg\sin(\theta) + \frac{\rho C_x S_f V(t)^2}{2} + MgC_R \tag{4}$$

The total energy consumed by a vehicle can be evaluated in terms of time integral function of the power. It can beexpressed by the following equation

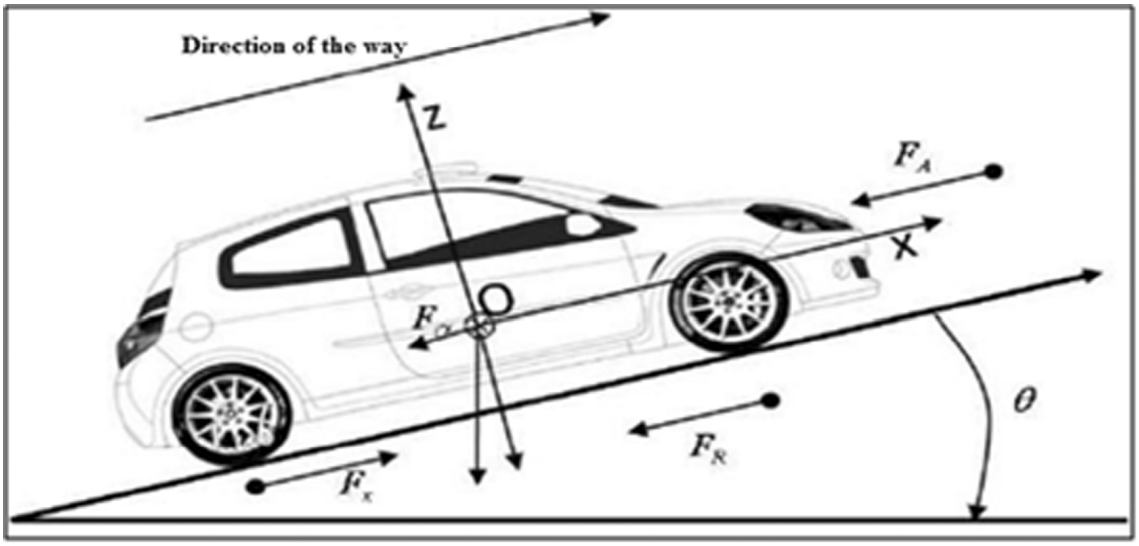

Figure 2: Forces acting on the vehicle

$$W(t) = F_x(t)\,d = \int F_x(t)\,V(t)\,dt \tag{5}$$

Where d is the distance travelled by the vehicle.

The mechanical power provided to the wheels is equal to:

$$P_m(t) = \frac{dW(t)}{dt} = F_x V(t)$$

$$P_m(t) = V(t)\,M\frac{dV(t)}{dt} + Mg\sin(\theta) + \frac{\rho C_x S_f V(t)^2}{2} + MgC_R \tag{6}$$

4. PMSM MODEL

The permanent magnet synchronous motor model is developed using d-q Park transformation. This representation is necessary because the inputs and the outputs of the model of the synchronous machine are expressed in the(a, b, c) frame.

The Park transformation is used to convert voltage, flux and current from the (a, b, c) frame to the (d, q) frame (Fig. 3) [10].

The electrical and mechanical equations of the synchronous machine are expressed as follows:

$$\begin{cases} \dfrac{d}{dt}I_{sd} = \dfrac{1}{L_{sd}}\left(V_{sd} - R_s I_{sd} + \omega L_{sd} I_{sd}\right) \\ \dfrac{d}{dt}I_{sq} = \dfrac{1}{L_{sq}}\left(V_{sq} - R_s I_{sq} - \omega L_{sq} I_{sq} + \omega\varphi_f\right) \\ Ce = \dfrac{3}{2}p\left[\left(L_{sd} - L_{sq}\right)I_{sd} I_{sq} + \varphi_f I_{sq}\right] \\ J\dfrac{d\Omega}{dt} = Ce - Cr - f\Omega \end{cases} \tag{7}$$

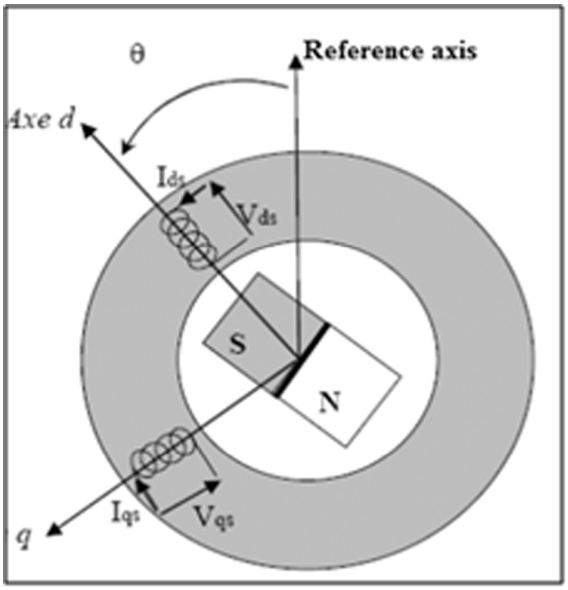

Figure 3: Equivalent Diagram of a PMSM in the Park frame

Where:

R_s : Resistance of a stator phase

L_{sd} : The cyclicinductance of the d axis

L_{sq} : Thecyclicinductance of the axis q

Φ_f : Magnetic flux

C_e : Electromagnetic torque provided by the PMSM motor,

C_r : Load torque

J : Motor Inertia

Ω : Mechanical speed of the motor,

P : number of pole pairs.

5. FUEL CELL MODEL

A fuel cell is an energy conversion system that converts chemical energy into electrical energy without any thermal or mechanical process. The operating principle of a fuel cell is described by a chemical reaction that reacted hydrogen and oxygen to produce electricity, heat and water, according to the chemical reaction given by eq. (8) [8]-[14].

$$2H_2 + O_2 \rightarrow H_2O + electricity + heat \tag{8}$$

There are many fuel cell models; each model has its own specificities and benefits, according to the phenomena studied. The chosen modelshould be simple and accurate.

Indeed, this work presents an electrochemical model which can be used to predict the fuel cell behavior in static and dynamic conditions[5]-[7]-[4].

The fuel cell voltage depends on the partial pressures of hydrogen and oxygen, the chemical reaction temperature of the membrane hydration and the output current. It is defined by the following equation [8]-[12]-[14].

$$V_{FC} = E_{Nernst} - V_{act} - V_{ohm} - V_{con} \tag{9}$$

Where:

$$E_{Nernst} = 1.229 + \frac{RT}{n_e F} \ln\left(\frac{PH_2\sqrt{PO_2}}{PH_2O}\right) \tag{10}$$

$$\Delta V_{Act} = \frac{RT}{n_e F} \ln\left(\frac{i_{FC}}{i_o}\right) \tag{11}$$

$$\Delta V_{Ohm} = R_{FC} i_{FC} \tag{12}$$

$$\Delta V_{Con} = -\frac{RT}{\alpha n_e F} \ln\left(1 - \frac{i_{FC}}{i_l}\right) \tag{13}$$

E_{Nernst} : the average thermodynamic potential of each unit cell.

V_{Act} : the activation voltage drop.

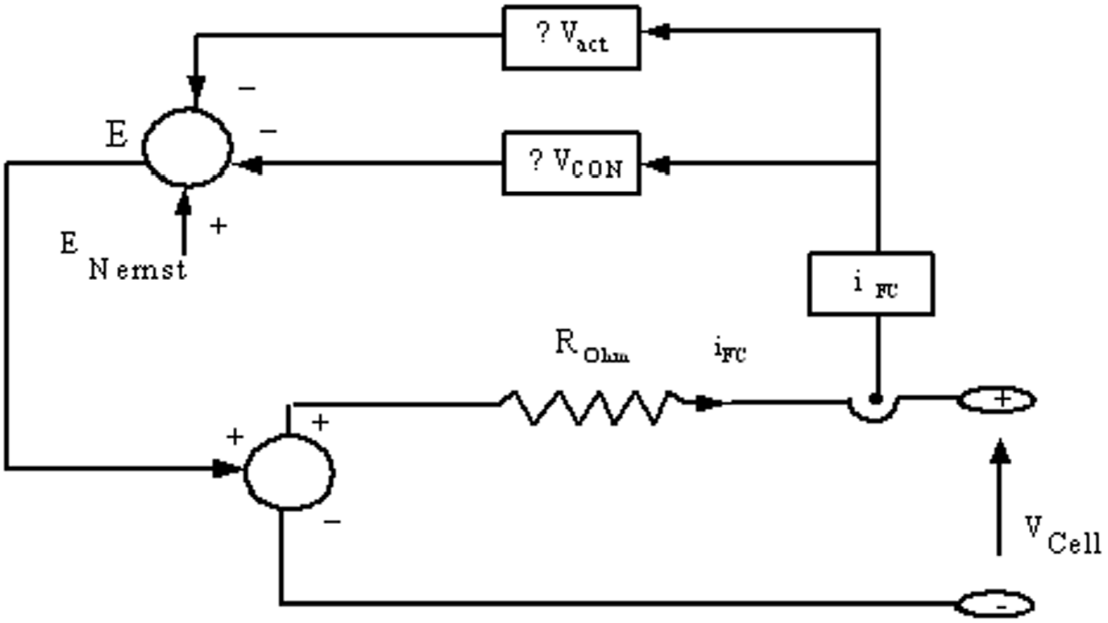

Figure 4: The electrical model of a fuel cell

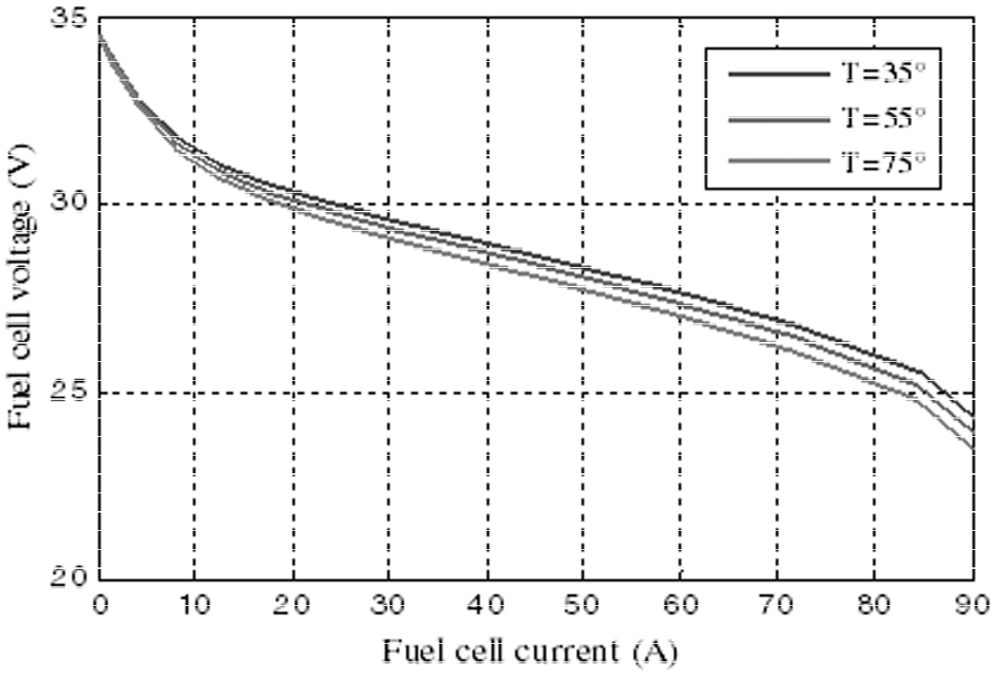

Figure 5: Polarization curve at different temperatures.

V_{Ohm} : the Ohmic voltage drop.

V_{Con} : the concentration voltage drop.

The polarization curve of a fuel cell is that which represents the battery voltage as a function of current output. This curve is presented for different temperature values. Fuel cell polarization curves increase with increasing of operating temperature such as shown in Fig.5.

6. FUEL CELL DC-DC CONVERTERMODEL

Basically, DC-DC converters can be divided into two categories depending on using the galvanic insulation or not: non-isolated converter or isolated converter as the noisolated converters are simple, but they require

an input inductance to limit the current ripple in the components. But, in many cases, isolation between the input and the output is required, because of operating specifications or for security reasons. For this reason the use of the isolated DC-DC converters. The chosen topology is divided in three parts: a high frequency DC-AC converter, a high-frequency transformer and an AC-DC converter as shown in Fig. 6 [2]-[3]-[8].

The converter is consists of:

- Full bridge side fuel cell, composed by bidirectional switches ((T11, D11), (T12, D12), (T13, D13) and (T14, D14)).
- Full bridge side high voltage, it is composed by unidirectional switches D1, D2, D3 and D4.
- The resonant filter consists of capacitor (Cr) and inductance (Lr). It's used to minimize the switching losses.
- Two planar transformers in high frequency, plays an important role in this topology. It provides both galvanic isolation and energy storage through winding leakage inductance. The primary is coupled in parallel and the secondary are in series, [11]-[12]-[13]-[14].

The bridge side fuel cell is controlled to generate a high frequency voltage wave format its transformers. Ts and d denotes respectively the switching period and the controlled duty ratio. Fig.7 shows the switching

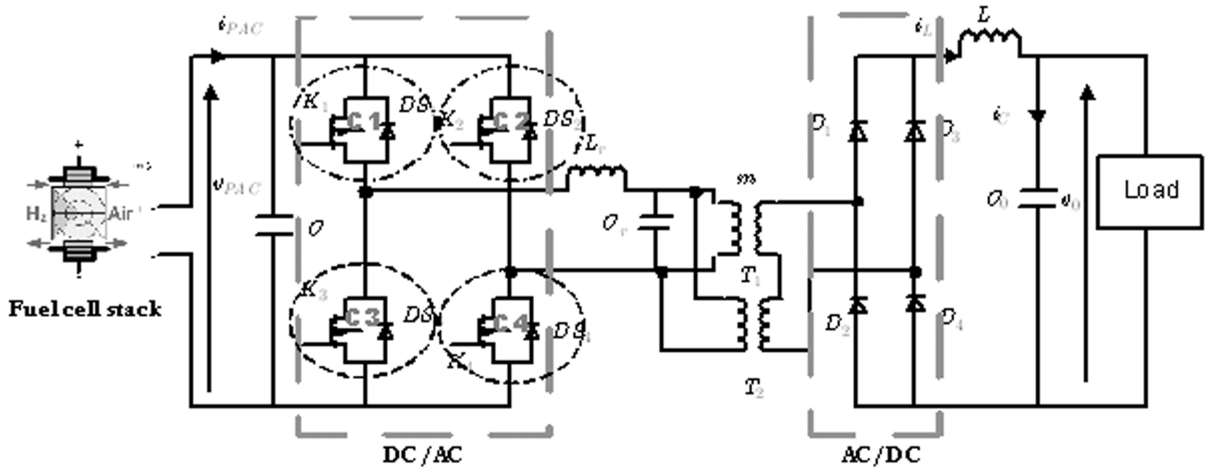

Figure 6: Topology of the converter

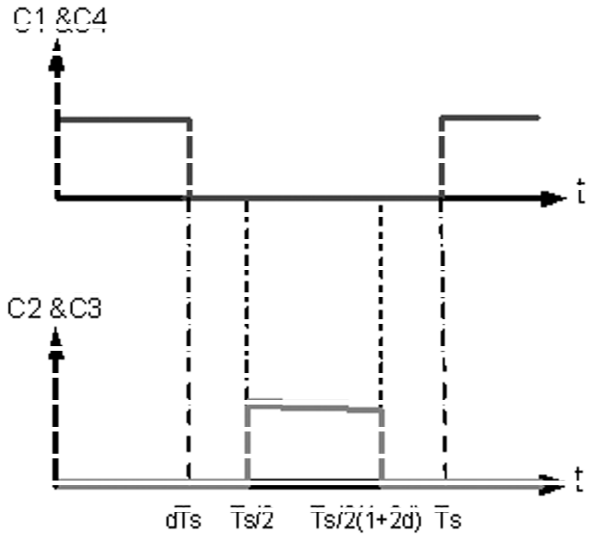

Figure 7: Waveforms of the gates signal of the converter

state converter. C1 C2 C3and C4 denotes respectively, the control signals of the switches K1, K2, K3and K4.

There is two stages:

- **Stage 1:** When the fuel cell has been started up, the power flows from the fuel cell to the load through two diagonally transistors, resonant circuit, planar transformers and two diodes. The equivalent circuit is as follows.

If all impedance is transferred to the secondary winding, the equivalent circuit becomes the following.

Where:

$$\begin{cases} R_{eq1} = 2r_D + 2m^2 r_T \\ L_{eq1} = L + m^2 L_r \\ C_{eq1} = C_o + \dfrac{C_r}{m^2} \end{cases} \tag{14}$$

Using the Kirchhoff laws we obtain:

$$\begin{cases} \dfrac{di_L}{dt} = -\dfrac{R_{eq1}}{L_{eq1}} i_L(t) - \dfrac{1}{L_{eq1}} v_o + \dfrac{2m}{L_{eq1}} V_{pac} \\ \dfrac{dv_o}{dt} = \dfrac{1}{C_{eq1}} i_L(t) - \dfrac{1}{C_{eq1}} v_o \end{cases} \tag{15}$$

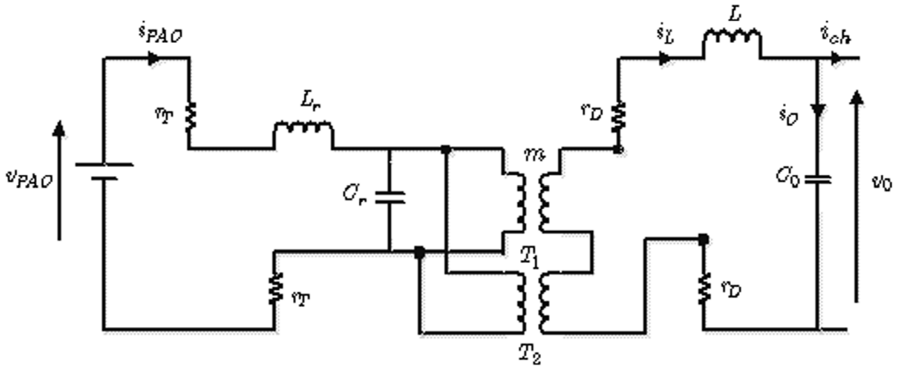

Figure 8: Equivalent circuit (Stage1)

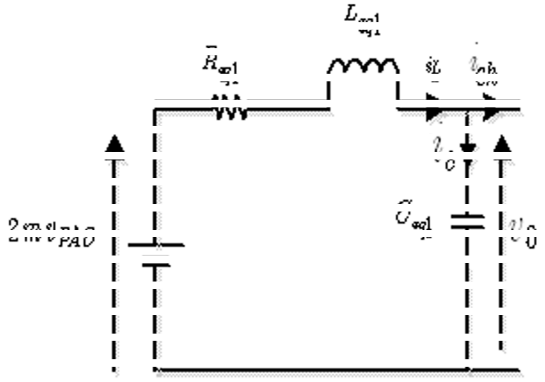

Figure 9: Equivalent circuit in secondary side

The state model can be writing by Eq. (10):

$$\begin{pmatrix} \frac{di_L}{dt} \\ \frac{dv_o}{dt} \end{pmatrix} = \begin{pmatrix} -\frac{R_{eq1}}{L_{eq1}} & -\frac{1}{L_{eq1}} \\ \frac{1}{C_{eq1}} & -\frac{1}{C_{eq1}} \end{pmatrix} * \begin{pmatrix} i_L \\ v_o \end{pmatrix} + \begin{pmatrix} \frac{2m}{L_{eq1}} \\ 0 \end{pmatrix} * V_{pac} \tag{16}$$

Therefore, the state model during dT_s is:

$$\begin{cases} \dot{x} = A_1 x + B_1 u \\ y = C_1 x \end{cases} \tag{17}$$

With:

$$\begin{cases} A_1 = \begin{pmatrix} -\frac{R_{eq1}}{L_{eq1}} & -\frac{1}{L_{eq1}} \\ \frac{1}{C_{eq1}} & -\frac{1}{C_{eq1}} \end{pmatrix} \\ B_1 = \begin{pmatrix} \frac{2m}{L_{eq1}} \\ 0 \end{pmatrix} \\ C_1 = \begin{pmatrix} 0 & 1 \end{pmatrix} \end{cases} \tag{18}$$

- **Stage 2:** The inductor current cannot be equal to zero instantaneously, so the two diodes are in conduction mode all switches are off. The equivalent circuit is show by Fig. 10

  The equivalent circuit of the DC-DC converter referred to secondary winding is show in Fig. 11

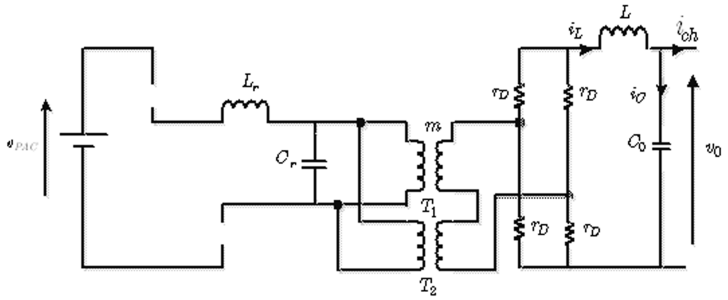

Figure 10: Equivalent circuit (Stage 2)

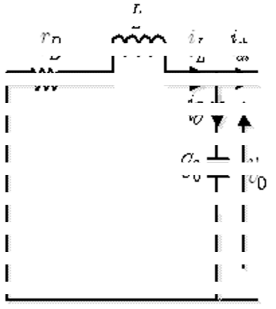

Figure 11: Referred secondary of the equivalent circuit

During the interval [*dTs, Ts*], the state space model and matrices are:

$$\begin{cases} \dot{x} = A_2 x + B_2 u \\ y = C_2 x \end{cases} \tag{19}$$

Using Kirchoff law, we obtain:

$$\begin{cases} \dfrac{di_L}{dt} = -\dfrac{r_D}{L} i_L(t) - \dfrac{1}{L} v_o \\ \dfrac{dv_o}{dt} = \dfrac{1}{C_o} i_L(t) - \dfrac{1}{C_o} v_o \end{cases} \tag{20}$$

$$\begin{cases} A_2 = \begin{pmatrix} -\dfrac{r_D}{L} & -\dfrac{1}{L} \\ \dfrac{1}{C_o} & -\dfrac{1}{R_{ch} C_o} \end{pmatrix} \\ B_2 = \begin{pmatrix} 0 \\ 0 \end{pmatrix} \\ C_2 = (0 \quad 1) \end{cases} \tag{21}$$

The last half cycle is identical to the first half cycle, so during switching period, stage 1 and stage 2 are repeated twice. Finally, the averaged model state equation can be obtained:

$$\begin{cases} \dot{x} = Ax + Bu \\ y = Cx \end{cases} \tag{22}$$

Where:

$$\begin{cases} A = 2d A_1 + (1-2d) A_2 = \begin{pmatrix} -\dfrac{2d R_{eq1}}{L_{eq1}} - \dfrac{(1-2d) r_D}{L} & -\dfrac{2d}{L_{eq1}} - \dfrac{(1-2d)}{L} \\ \dfrac{2d}{C_{eq1}} + \dfrac{(1-2d)}{C_o} & -\dfrac{2d}{R_{ch} C_{eq1}} - \dfrac{(1-2d)}{R C_o} \end{pmatrix} \\ B = 2d B_1 + (1-2d) B_2 = \begin{pmatrix} \dfrac{4md}{L_{eq1}} \\ 0 \end{pmatrix} \\ C = 2d C_1 + (1-2d) C_2 = \begin{pmatrix} 0 \\ 1 \end{pmatrix}^t \end{cases} \tag{23}$$

Average large signal circuit model is often derived as shown in Fig. 12.

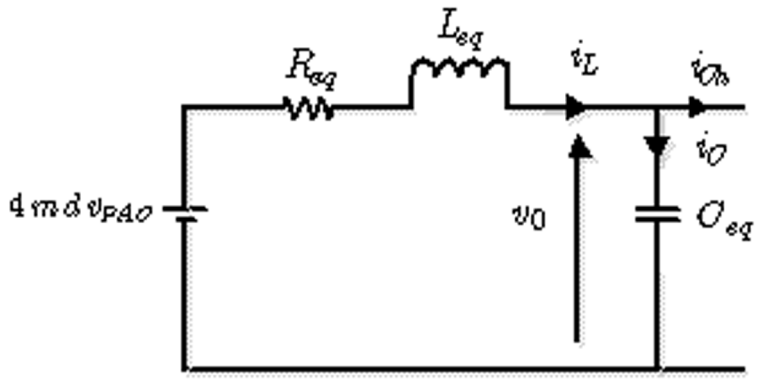

Figure 12: Equivalent circuit model

7. VECTOR CONTROL OF THE PERMANENT MAGNET SYCHRONOUS MOTOR

In DC motors, the flux and torque producing currents are orthogonal and can be controlled independently. The magneto motive forces, developed by these currents are also held orthogonal.Hence the flux is only dependent on the field winding current. If the flux is held constant, then the torquecan be controlled by the armature current. For this reason DC machines are said to have decoupled orhave independent control of torque and flux.In AC machines, the stator and rotor fields are not orthogonal to each other. The only current that can becontrolled is the stator current. Field Oriented Control is the technique used to achieve the decoupledcontrol of torque and flux by transforming the stator current quantities (phase currents) from stationaryreference frame to torque and flux producing currents components in Park rotating reference frame.The inverse stator current component Iq control the required torque and the direct currentcomponent Id of the stator current control the flux magnetite. [15]-[17]-[18]. The Oriented Field control strategy of the PMSM is given by Fig. 13,[19]-[21].

The voltage supply is obtained by imposing the reference voltage standards input to the control of the inverter. These voltages allow determining the cyclic ratios on the arms of the inverter, so that the voltage

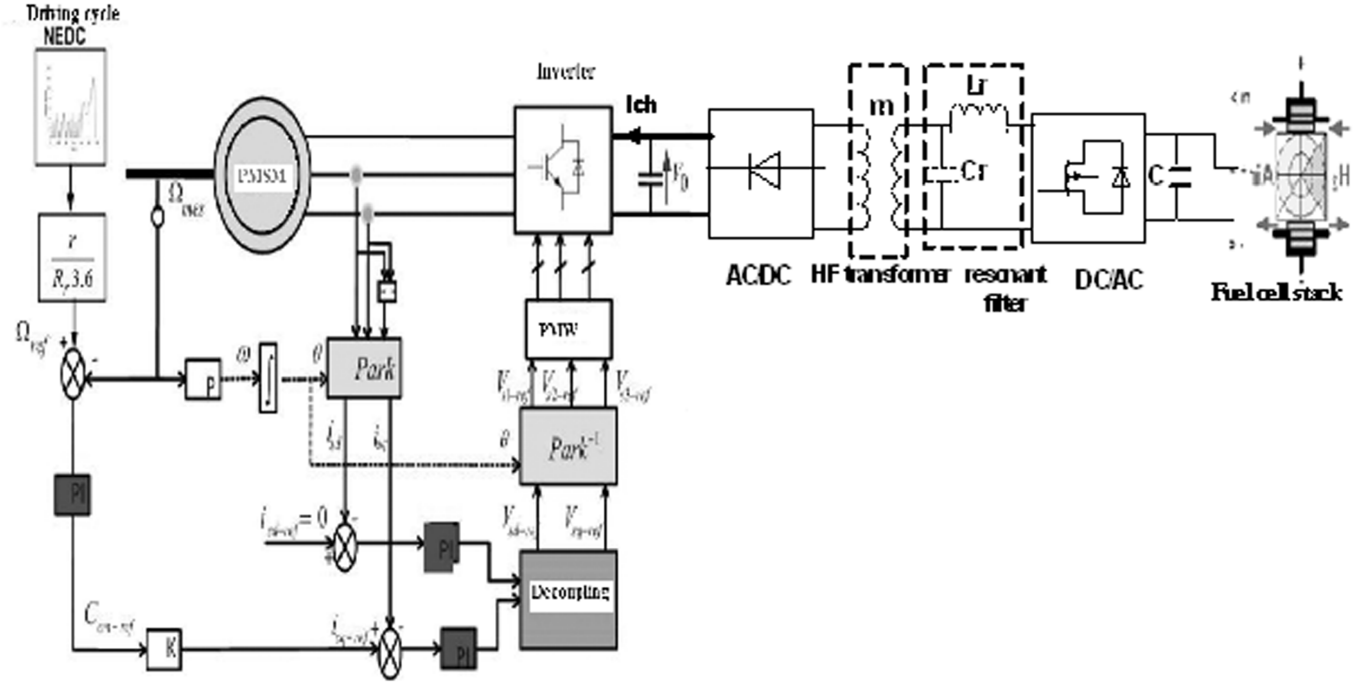

Figure 13: Structure of the Field Vector Control of the PMSM

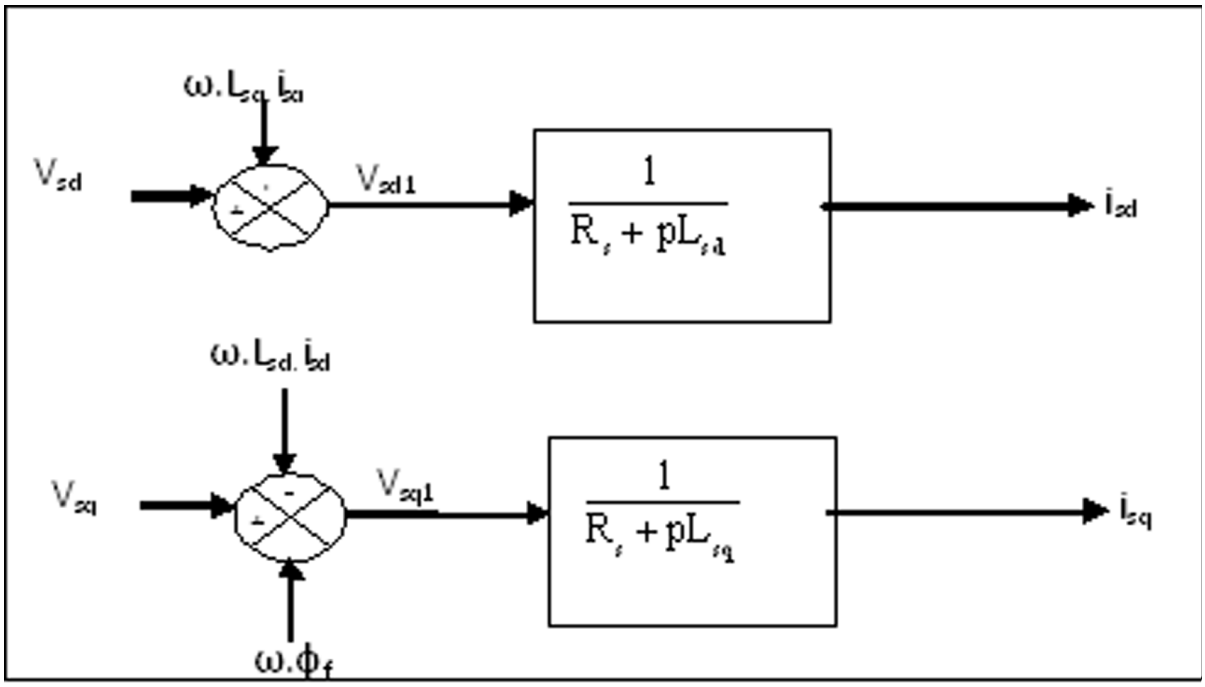

Figure 14: Coupling of the two stator voltage

delivered by this inverter at the stator winding of the PMSM is closest to possible reference voltage standards. But, we must define the terms of compensation, because in the stator equations, there are terms of coupling between the d axes and q axis voltage components (Fig.14) [19]-[20]-[22].

The voltages Vsd and Vsq depend at the same time on both currents on the axes 'd' and 'q', thus lead to establish adecoupling. This decoupling is based on the introduction of compensatory terms $\mathbf{e}_{sd}$ and $\mathbf{e}_{sq}$.

$$\begin{cases} e_{sd} = \omega L_{sq} I_{sq} \\ e_{sq} = \omega \left(L_{sd} I_{sd} + \varphi_{sf} \right) \end{cases} \tag{24}$$

From the previous equations we have:

$$\begin{cases} V_{sd} = V_{sd1} + e_{sd} \\ V_{sq} = V_{sq1} + e_{sq} \end{cases} \tag{25}$$

With:

$$\begin{cases} V_{sd1} = \left(R_s + pL_{sd} \right) I_{sd} \\ V_{sq1} = \left(R_s + pL_{sq} \right) I_{sq} \end{cases} \tag{26}$$

8. SIMULATION RESULTS

The simulation results are formed onthe energy conversion systemwhich containsfuel cell, DC/DC converter andmagnet synchronous motor in which these characteristics were given in table I and supplied with a controlled inverter according to the principle of vector PWM. For purposes of the simulation and for reproducing a road section with different driving conditions is used in the standardized European speed cycle (NEDC), Fig.15 [17]-[18].

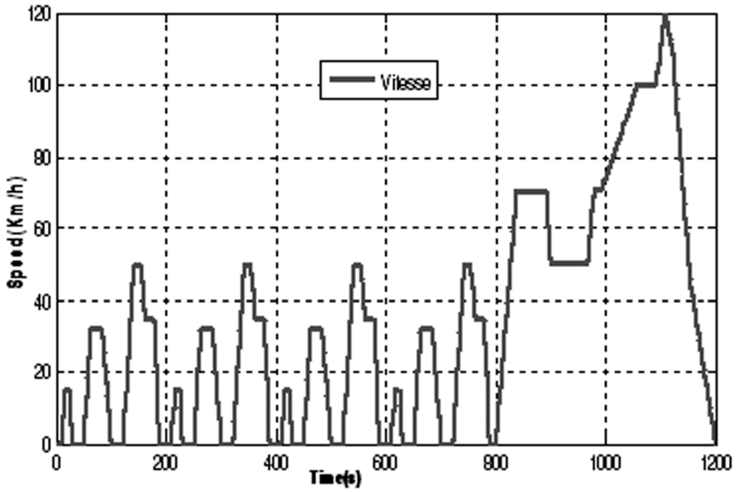

Figure 15: Normalized European Cycle speed (NEDC)

Table 1
Fuel cell parameters

Parameter Name			*Parameter Value*
Temperature	T	328 °K	
Partial pressure of Hydrogen	PH2		1.5 atm
Partial pressure of Oxygen	PO2		1 atm
Partial pressure of Water	PHO2		1 atm
Exchange current	i0		0.002A
Cell area	A		0.0825m^2
Limiting current	iL		100A

Table 2
Parameters of the motor

Parameter Name		*Parameter Value*
Stator resistor	Rs	4 Ω
Stator inductance	Ls	0.0025 H
Poles pairs	P	4
Flux of permanent magnet	φf	0.053Wb
Rotational inertia	J	9e-7 Nm/A
Rated speed	Ω	rad/s
DC voltage	U_{DC}	540 V
friction coefficient	f	0 Nm/rad/s

Table 3
Parameters of the VEHICLE

Parameter Name		*Parameter Value*
Vehicle mass	M	300 kg
Rolling resistance coefficient	CR	0.001
Vehicle front section	Sf	1 m^2
Gravitational field	g	9.81 ms-2
Slope	tan(ômax)	10%
Radius of the wheels	Rr	0.14 m
Volume density of air	ρ	1.2 Kg/m^3

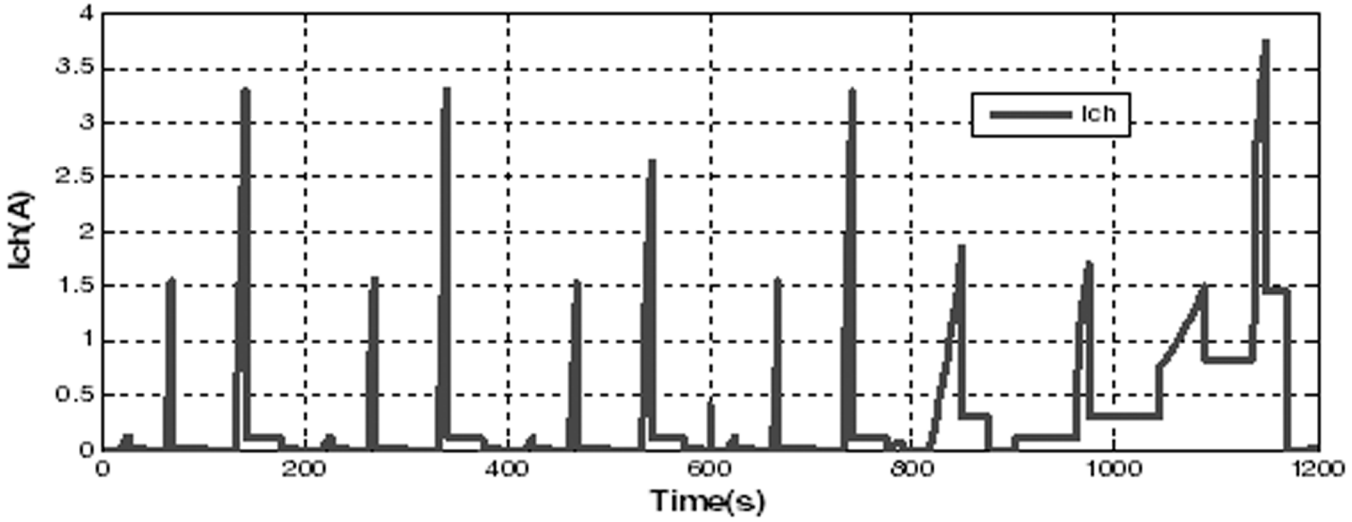

Figure 16: Current profile I_{ch}

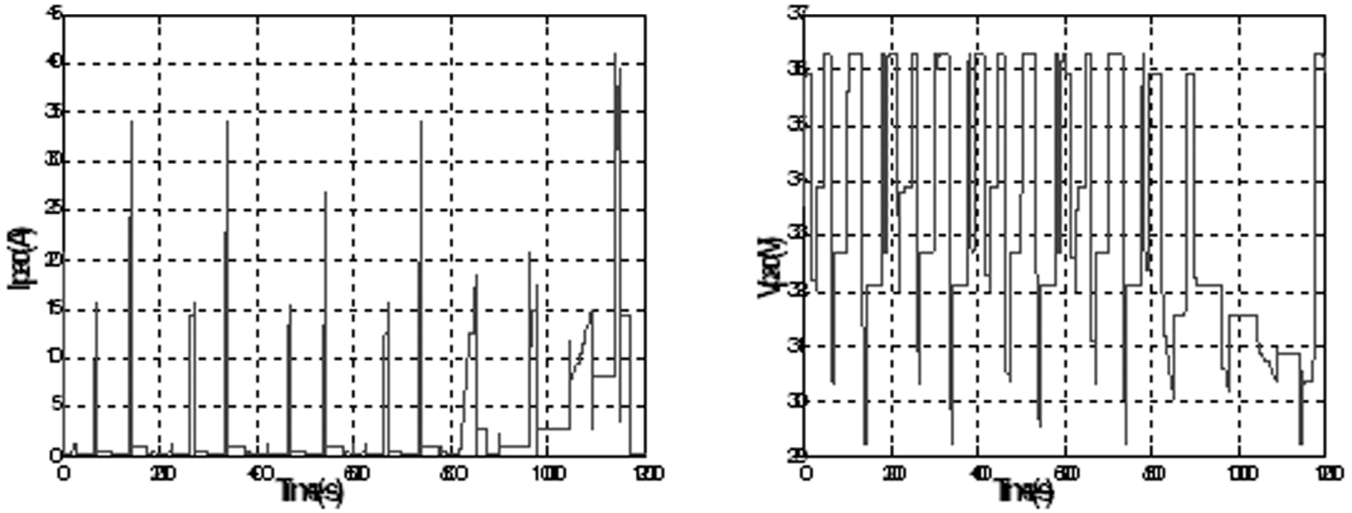

Figure 17: Current and voltage of the fuel cell stack

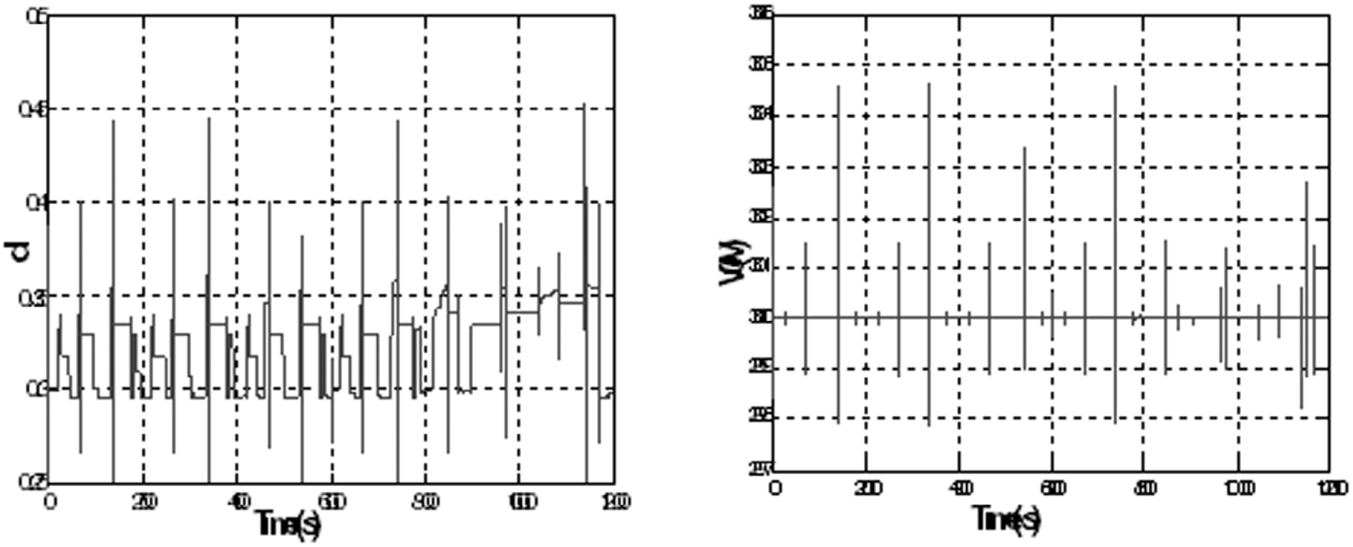

Figure 18: Duty Cycle report and DC bus voltage

The profile of the load current imposed is presented by Fig.16. The current variation requested by the load causes the change in current flow through the fuel cellstack. The PPIC resistance causes a voltage drop. The Fig. 17 shows the current and the voltage of the fuel cell.

When the current absorbed by the load increases,the voltage of the fuel cell stack decreases. In order to maintain the voltage of continuous bus constant, it must increase the cyclic report as shown in the Fig.18.

Fig. 19 shows the evolution of the speed of that vehicle motion and angular speed of the permanent magnet synchronous motor. It is observed that this last shows oscillations. Fig. 20 presents the evolution of the electric power provided by the permanent magnet synchronous motor. The results got in digital simulation highlight the performances of the control system. The torque Ce and the Iq current have the similar wave forms. The current Id riches it's reference.

9. CONCLUSION

This paper presents the sizing of different components of the energetic conversion system used in electric vehicle. We started with the vehicle mechanical model. The established model allowed us to calculate the

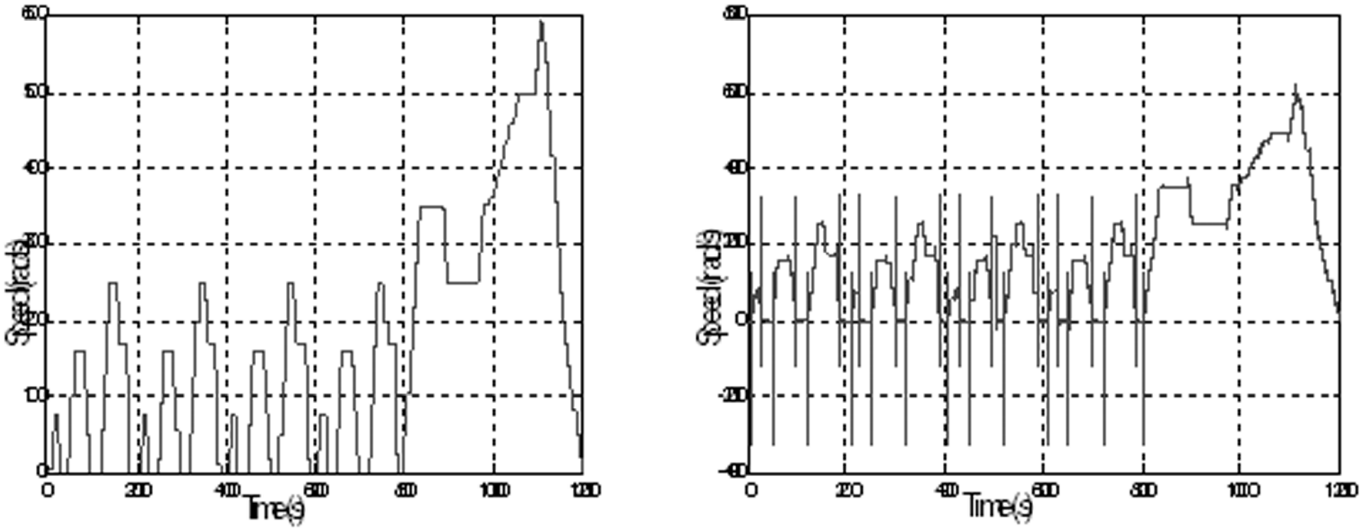

Figure 19: Vehicle and Motor speeds

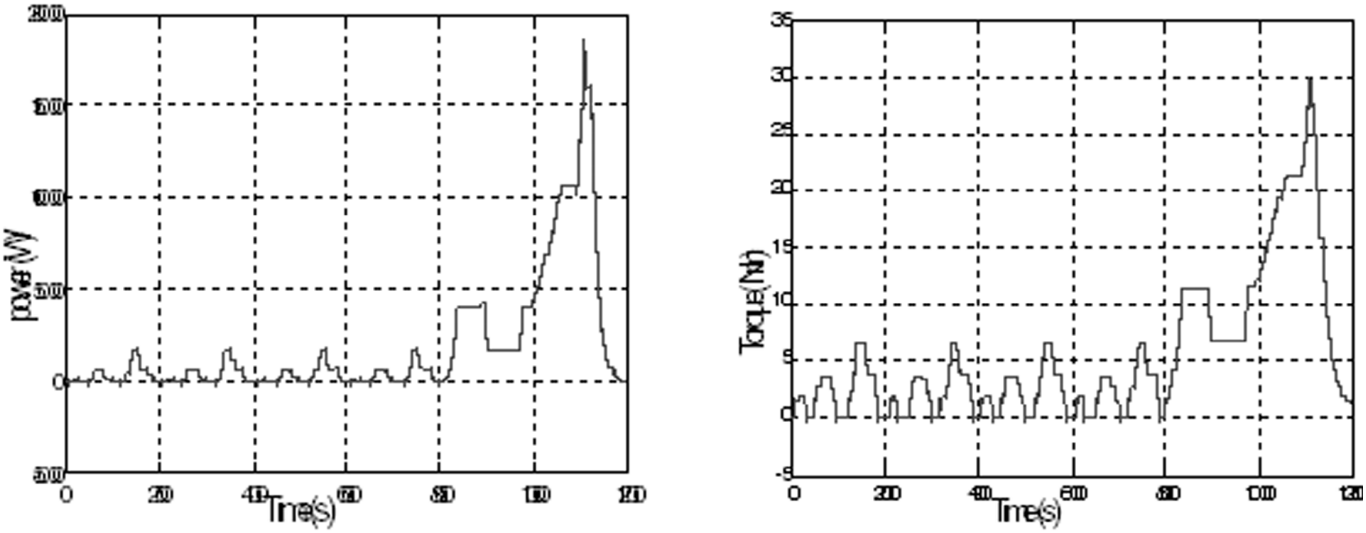

Figure 20: Motor power and Electromagnetic torque

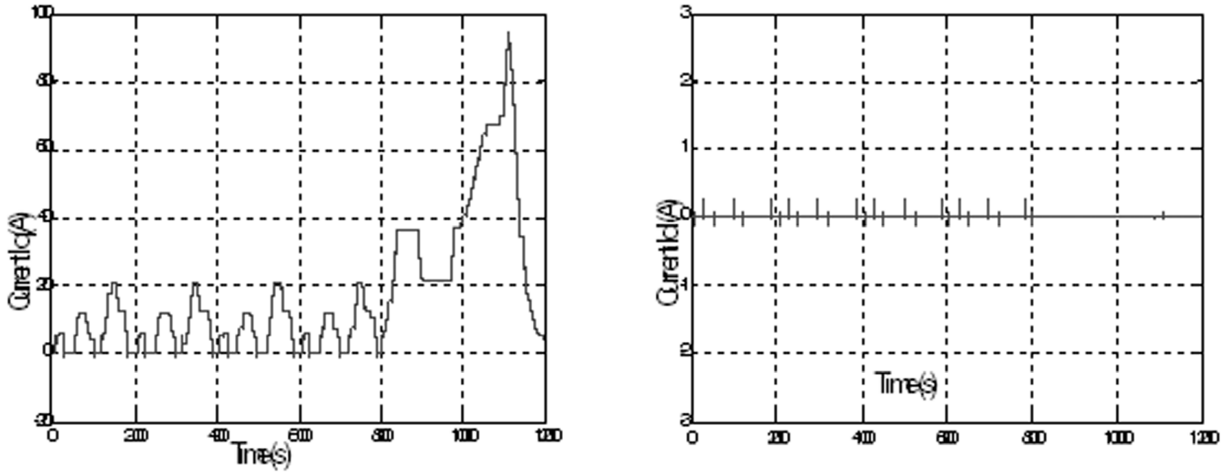

Figure 21:Direct and inverse component Idand Iq of the stator currents

required power. Then we determine the characteristic of the permanent magnet synchronous motor to taking into account the overall performance of the energy conversion system of the concerned vehicle. Then a simple model of the stack in function was put, a point on the goal to characterize the voltage of the fuel stack in function of the average power requested by the vehicle. This model calculates the battery voltage as function of current debited the temperature of the stack fuel as well as the partial pressures of the hydrogen and oxygen.

The fuel stack is characterized by a source of low voltage. For this purpose, that it is connected to the DC bus via a DC-DC converter to operate at high frequency in order to minimize the weight. It also used a DC-ACconverter which interfaces the DC bus and the PMSM whose control used is the vector pulse width modulation technique.

The simulation results under Simulink/Matlab show the current absorbed by the load increases, the voltage of the fuel cell stacks decreases. In order to maintain the voltage of the DC bus constant, the duty cycle of the DC/DC convertershould beincreased. The torque and the q-axis stator current have the same shape and the direct current Id follows it's reference. The proposed control scheme provides acceptable dynamic and robust responses.

REFERENCES

[1] M. Amari, J.Ghouili and F. Bacha, "New high frequency unidirectional DC-DC converter for fuel-cell electrical vehicles," 24th Canadian Conference on Electrical and Computer Engineering (CCECE-2011), pp. 1451-1458, 2011.

[2] G. Garci, G.Oggier and A. Oliva, "Modulation strategy to operate the dual active bridge dc-dc converter undersoft switching in the whole operating range," *IEEE Transactions on Power Electronics*,**26** (4), 1228-1236,2011.

[3] M. Amari, F. Bacha, J.Ghouili and I.Elgharbi, "Design and analysis of high frequency dc-dc converters for fuel cell and super-capacitor used in electric vehicle," *International Journal of Hydrogen Energy*,**39** (4),1580-1592, 2014.

[4] Z. Zhang, R. Pittini, M.Andersen and O.Thomsen, "Areview and design for power electronics converters for fuel cell hybrid system applications," *Energy Procedia*,**20**, 301-310,2012.

[5] R. Seyezhaai and B.L. Mathum, "Mathematical modeling of proton exchange membrane fuel cell," *International Journal of Computer Applications*, **20** (5), 1-6, 2011.

[6] H. Qin and J.W. Kimball, "Generalized average modeling of dual active bridge dc-dc converter," *IEEE Transactions on Power Electronics,***27** (4),2078-2084, 2012.

[7] B. Vural, O. Erdinc and M. Uzunoglu, "Parallel combination of FC and UC for vehicular power systems using a multi-input converter based power interface,"*Energy Conversion and Management*, **51**, 2613-2622, 2010.

[8] D.N.S. Saranya, A.R. Vijay Babe, G. Srinivsa Rao, Y.R. Tagore and N. Bharath Kumar ,"Fuel cell powered bidirectional dc-dc converter with fuzzy logic controller for electric vehicle applications," *International Journal of Control Theory and Applications*, 8 (1),109-120, 2015.

[9] L.S. Yang and T.J. Liang , "Analysis and implementation of a novel bidirectional dc-dc converter," *IEEE Transactions on Industrial Electronics,*59 (1), 422-434, 2012.

[10] A. MohamdiJahandizi and M. Hadad. Zarif, "Intelligent nonlinear control of IPMSM using Belbic," *International Journal of Control Theory and Applications,* **7** (1), 21-34, 2014.

[11] F. Abddous, "Fuel cell DC/DC converter control by sliding mode method," *WASET Journal*,**49**, 1011-1015, 2009.

[12] A. Kirubakaran, S. Jain and R.K.Nema, "The PEM fuel cell system with DC/DC boost converter: Design, modeling and simulation," *International Journal of Recent Trends in Engineering,* **1** (3), 157-162, May 2009.

[13] O. Krykunov, "Comparison of the DC/DC-Converters for fuel cell applications,"WASET Journal*,* **27**, 425-434, 2007.

[14] M.Belatel, F.Z.Aissous and F.Ferhat, "Contribution à l'étude d'une pile à combustible de type PEMFC utilisée pour la production d'énergie électriqueverte," *Revue des Energies Renouvelables,* Vol. **15** (1), 13-28, 2012.

[15] K. Jaber, B. Ben Saleh, A. Fakhfakh and R. Neji, "Modeling and Simulation of electricalvehicle in VHDL-AMS," 16th IEEEInternational Conferenceon,Electronics, Circuits andSystems (ICECS- 2009), pp. 908-911,2009.

[16] P.H.Nguyen, E.Hoang,M.Gabsi and M.Lècrivain, "Caractéristique sur cycles des machines synchrones à concentration de flux pour une application véhicule hybride,"*European Journal of Electrical Engineering*, **14** (2), 309-329, 2011.

[17] P.H. Nguyen, E. Hoang, M. Gabsi, L. Kobylansk and D. Comdamin, "Permanent magnet synchronous machines:Performances during driving cycle of a hybrid electric vehicle application," *IEEE International Symposium on Industrial Electronics*,pp. 1432-1438, Bari,Italie, July 2010.

[18] P.H. Nguyen, E. Hoang and M. Gabsi, "Performance synthesis of permanent magnet synchronous machines during the driving cycle of a hybrid electric vehicle",*IEEE Transactions on Vehicular Technology*, **60** (5),1991-1998, 2011.

[19] A. Khlaief, M. Bendjedia and M. Boussak, "A nonlinear observer forhigh-performance sensorless speed control of IPMSM drive," *IEEE Transactions on Power Electronics*, **27** (6), 3028–3040, 2012.

[20] A. Taghvipour, N.L. Azad and J. Mcphee, "Real-time predictive control strategy for a plug-in hybrid electric powertrain," *Mechatronics*, **29**, 13–27, 2015.

[21] X. Wang, H. He, F. Sun and J. Zohang, "Application study on the dynamic programmingalgorithmfor energy management of plug-in hybrid electric vehicles," *Energies,* **8** (4), 3225–3244, 2015.

[22] F. Salem, "Modeling and control solutions for electric vehicles," *European Scientific Journal,* **9** (15), 221–240, 2013.

[23] S. Vaidyanathan, "A novel 3-D conservative chaotic system with a sinusoidal nonlinearity and its adaptive control", *International Journal of Control Theory and Applications*, **9** (1), 115-132, 2016.

[24] S. Vaidyanathan and S. Pakiriswamy, "A five-term 3-D novel conservative chaotic system and its generalized projective synchronization via adaptive control method", *International Journal of Control Theory and Applications*, **9** (1), 61-78, 2016.

[25] S. Sampath and S. Vaidyanathan, "Hybrid synchronization of identical chaotic systems via novel sliding control method with application to Sampath four-scroll system," *International Journal of Control Theory and Applications*, **9** (1), 221-235, 2016.